



## Electrochemical Hybrid Supercapacitors Based on Activated Carbon and Iron Oxides

S. Veleva<sup>1</sup>, . Stoyanova<sup>2</sup>, R. Raicheff<sup>3</sup>, D. Kovacheva<sup>4</sup>, M. Mladenov<sup>5</sup>  
<sup>1,2,3,5</sup> Institute of Electrochemistry and Energy Systems – BAS, Sofia 1113, Bulgaria.  
<sup>4</sup> Institute of General and Inorganic Chemistry – BAS, Sofia 1113, Bulgaria.

### Abstract

Hybrid lithium battery-supercapacitor is developed using nanosized electrode materials – activated carbon and iron oxides (magnetite and hematite) and a non-aqueous electrolyte. The hybrid cell is assembled by an electrode of activated carbon, a composite electrode with activated carbon matrix and addition of 50 wt.% Fe<sub>3</sub>O<sub>4</sub> or Fe<sub>2</sub>O<sub>3</sub>. Symmetric supercapacitor cell, composed by two identical electrodes of activated carbon is also assembled and tested for comparison.

The supercapacitor cells are subjected to charge/discharge cycling test under galvanostatic conditions at different current loads and continuous cycling. The hybrids supercapacitors developed, especially the magnetite based cell, demonstrate high current efficiency (up to 95%) and specific capacity higher (with 20-50%) than the capacities of the basic symmetric capacitor (about 50 Fg<sup>-1</sup>) as well as stable capacity behaviors at prolong cycling. The results prove the possibility of application of magnetite and hematite as electrochemically active material for hybrid lithium battery–supercapacitor systems.

**Keywords:** Hybrid Supercapacitors; Activated Carbon; Iron Oxides; Non-Aqueous Electrolyte.

### 1. Introduction

The growing interest to the electrochemical supercapacitors as energy storage and power delivery technologies in the fields of renewable energy systems, hybrid electric vehicles, portable electronics and communication devices are attributed to their remarkable advantages in comparison to the conventional electrochemical power sources – batteries and fuel cells, such as high power capability, high rate of charge/discharge, high efficiency, low level of heat emission, environmental friendliness and practically unlimited cycle life [1-5].

The first electrochemical supercapacitors developed are double-layer symmetrical capacitors composed by two identical carbon electrodes and an organic electrolyte. Porous carbons are among the most attractive materials for preparation of electrodes for electrochemical supercapacitors. The main advantage of those materials is the possibility to produce highly porous structures with high specific surface area as well as to develop various composite electrodes by adding electrochemically active components to carbon matrix [2, 5].

The integration of supercapacitors and batteries in energy storage and delivery systems gives a possibility to combine the high transient performance of the supercapacitors with high steady-state characteristics of the batteries. In order to improve the energy density while keeping long cycle life of the supercapacitors, hybrid electrochemical systems involving hybridization of a faradaically rechargeable battery-type electrode with an electrochemical double-layer capacitor-type electrode [e.g. asymmetric supercapacitors], are introduced. On this basis various hybrid capacitor configurations, consisting of activated carbon as a positive electrode and a negative electrode based on metal oxides (nickel, lead or manganese oxides) [6–8], conducting polymers [9] or Li intercalation oxides [10, 11], are suggested.

In previous our studies [12-15], it is shown that activated nanoporous carbon materials suitable for electrodes of electrochemical double-layer supercapacitors and for composite carbon-based electrodes of hybrid lithium battery-

supercapacitors can be synthesized from waste biomass [apricot stones and spent coffee grounds) or by carbonization of mixtures of coal tar pitch and furfural with subsequent hydrothermal and thermal treatments. Thus, capacitance values of up to  $70 \text{ Fg}^{-1}$  are obtained for symmetric supercapacitors assembled with two identical activated carbon electrodes and a non-aqueous electrolyte  $\text{LiPF}_6 - \text{DMC/EC}$  (dimethyl carbonate/ethylene carbonate mixture 1:1) or  $\text{Et}_4\text{NBF}_4 - \text{PC}$  (propylene carbonate) and about twice higher capacitance - for asymmetric battery-supercapacitors composed by an activated graphitized carbon electrode and a composite electrode with activated carbon matrix with addition of nanosized  $\text{Li}_4\text{Ti}_5\text{O}_{12}$  oxide, and a non-aqueous electrolyte ( $\text{LiPF}_6 - \text{DMC/EC}$  1:1), with high current efficiency of the charge/discharge and very good cycleability of both supercapacitor systems.

The iron oxides -  $\text{Fe}_2\text{O}_3$  and  $\text{Fe}_3\text{O}_4$  are promising electrode materials for lithium-ion batteries because of their low cost, simple manufacturing process, wide range of sources, non-toxicity and environmental friendliness, and mainly - large theoretical specific capacity of both oxides [16-22].

The pure iron oxide-based anode materials, however, suffer from a rapid capacity fading resulting from agglomeration and drastic volume change of the active materials upon continuous charge/discharge cycling, which may also lead to a partial destruction of the electrode. A variety of nanostructured composites with different matrices have recently been explored in an effort to circumvent these obstacles and achieve improved electrochemical properties, especially at high current rates. Carbon materials are usually selected as matrices for the nanocomposites [21-25] because the carbon phase can act as a buffer to absorb the volume changes and improve the structural stability of the electrode, increase the electrical conductivity, and ensure better electrochemical properties.

The objective of the present work is to develop an electrochemical hybrid lithium battery-supercapacitor composed by an activated carbon electrode, a composite electrode with activated carbon matrix and addition of  $\text{Fe}_2\text{O}_3$  or  $\text{Fe}_3\text{O}_4$  oxide, and a non-aqueous electrolyte.

## 2. Experimental

### 2.1. Synthesis of Nanosized $\text{Fe}_2\text{O}_3$ and $\text{Fe}_3\text{O}_4$

Activated nanoporous carbon (AC) and electrochemically active iron oxides -  $\alpha\text{-Fe}_2\text{O}_3$  (hematite) and  $\text{Fe}_3\text{O}_4$  (magnetite) are used as electrode materials for assembling of hybrid supercapacitor cells.

Nanosized magnetite and hematite are laboratory synthesized. Magnetite is obtained by sonochemical synthesis which is carried out by precipitation the corresponding metal hydroxides and their further decomposition to oxides under ultrasonic irradiation. As starting compounds  $\text{FeCl}_2 \cdot 6\text{H}_2\text{O}$ ,  $\text{Fe}(\text{NO}_3)_3 \cdot 9\text{H}_2\text{O}$  and  $\text{NaOH}$  in a molar ratio of 1:2:5 are used. The metal salts and  $\text{NaOH}$  are dissolved separately in an appropriate amount of distilled water. Coprecipitation occurs during addition of the mixed solution of iron salts to the solution of  $\text{NaOH}$ . The sonication is performed by 20 KHz, 750 W ultrasonic processor (Sonix, USA) in Ar-atmosphere for 1 hour. The resulting product is washed repeatedly with distilled water, filtered and dried at  $50^\circ\text{C}$ .

Hematite is obtained by solution combustion synthesis method. As starting reagents  $\text{Fe}(\text{NO}_3)_3 \cdot 9\text{H}_2\text{O}$  and sucrose (as fuel) in 3,2:1 molar ratio are used. Stoichiometric amounts of the reagents are dissolved in an appropriate amount of deionized water. The resulting solution is heated on a magnetic stirrer. Initially, the solution is dehydrated, and then the residue reaches the ignition point and ignites to release a large amount of heat and gases, while at the end of the reaction a fluffy powder is formed. After the synthesis the sample is grinded in agate mortar and subjected to thermal treatment at  $400^\circ\text{C}$  for 1 hour.

The activated carbon is a commercial product (TDA Research, USA).

### 2.2. Physicochemical Characterization of the Electrode Materials

The obtained synthetic oxide materials and activated carbon are structurally characterized by X-ray diffraction method. Powder X-ray diffraction patterns of iron oxides are collected within the range from  $10$  to  $80^\circ$  with a constant step of  $0.02^\circ$  on a Bruker D8 Advance diffractometer with  $\text{Cu K}$  radiation and a LynxEye detector. Phase identification is performed with the *Diffraplus* EVA using the ICDD-PDF2 Database. The powder diffraction patterns are evaluated with the Topas-4.2 software package using the fundamental parameters peak shape description including appropriate corrections for the instrumental broadening and diffractometer geometry. Unit cell parameters are obtained by whole powder XRD pattern fitting using as starting values the data taken from the files in ICDD-PDF2 (#79-416 for magnetite and #33-664 for hematite). Unit cell parameters, profile parameters as well as zero shift are varied to obtain a good fit with the experimental data. The mean crystallite sizes are determined using again the whole powder XRD pattern fitting mode of the program. For this purpose the integral line breadth approach for the generalized treatment of the domain size broadening -  $\tau_i = L_{vol} \cos \theta_i$  is employed, where  $\tau_i$  is the integral breadth of the diffraction line  $i$  and  $L_{vol}$  is the volume weighted mean column height.

The particle size and morphology are examined by Transmission electron microscopy (TEM) using a TEM JEOL 2100. The specimens are prepared by grinding the samples in an agate mortar and dispersing them in acetone by ultrasonic treatment for 5 min. A droplet of the suspension is dripped on standard carbon films on Cu grids.

The pore structure of the carbon used is investigated by nitrogen gas adsorption by means of porosimeter Micromeritics ASAP 2010. The adsorption isotherm of the sample at  $-196\text{ }^{\circ}\text{C}$  is recorded (not shown) and used to calculate the specific surface area, pore volumes and pore size distributions [13].

### 2.3. Preparation of Hybrid Supercapacitor Cells and Electrochemical Testing

The activated carbon and iron-oxides ( $\text{Fe}_2\text{O}_3$  or  $\text{Fe}_3\text{O}_4$ ) are used to fabricate electrodes for two types of electrochemical cells for capacity measurements. The first type is a symmetric supercapacitor cell using two identical electrodes from activated carbon and a non-aqueous electrolyte – lithium tetrafluoroborate ( $\text{LiBF}_4$ ) with organic solvent – ethylene carbonate and dimethyl carbonate (EC/DMC) mixture in ratio 1:1. The second one is a hybrid battery-supercapacitor cell is assembled by a composite electrode and an activated carbon electrode. The composite (negative) electrode is prepared of activated carbon matrix with addition (50 wt.%) of iron oxide –  $\text{Fe}_2\text{O}_3$  or  $\text{Fe}_3\text{O}_4$ . The positive electrode is made from the same activated carbon material. The same non-aqueous electrolyte –  $\text{LiBF}_4$ -EC/DMC (1:1) as in the symmetric supercapacitor cell is used.

The activated carbon is previously teflonised in well-established and tested procedure [14,15] using a mixture of 90 wt.% activated carbon powder and 10 wt.% polytetrafluoroethylene (PTFE binder – Aldrich, 60% suspension in water): heated at  $70\text{ }^{\circ}\text{C}$  with a magnetic stirrer for 2 hours, allowed to stand 12 hours and then dried at  $50\text{ }^{\circ}\text{C}$  [15]. By adding a conductive additive (5 wt.%) – natural graphite NG-7 to the electrode materials a paste is formed, which is glued to Al- or Cu- foil discs (surface area  $1,75\text{ cm}^2$ ). The sheet electrodes formed are dried in vacuum at  $120\text{ }^{\circ}\text{C}$  for 12 hours and pressed under pressure of  $200\text{ kg cm}^{-2}$ . The electrodes are soaked in the organic electrolyte under vacuum, mounted in a coin-type cell with a Glassmat separator and then the cell is filled with electrolyte in a dry box under argon atmosphere.

The capacitor cells are subjected to galvanostatic charge-discharge cycling over voltage of 0,6-2.4 V using an Arbin Instrument System BU-2000 [14,15]. The test program is carried out at constant current mode at different current loads (from 15 to  $500\text{ mA g}^{-1}$ ) with 10 cycles at every load and room temperature. Some cells are subjected to continuous cycling charge/discharge at current rate of  $60\text{ mA g}^{-1}$  up to 2000 cycles.

The value of the specific capacity  $I$  is obtained from the charge-discharge cycling measurements according to the following equation [26]:

$$C = 4 I t / m V \quad (1),$$

where  $I$ ,  $t$ ,  $V$  and  $m$  are respectively, the constant current applied, discharge (discharge) time, voltage interval of the charge or discharge and the total mass of the electrode material.

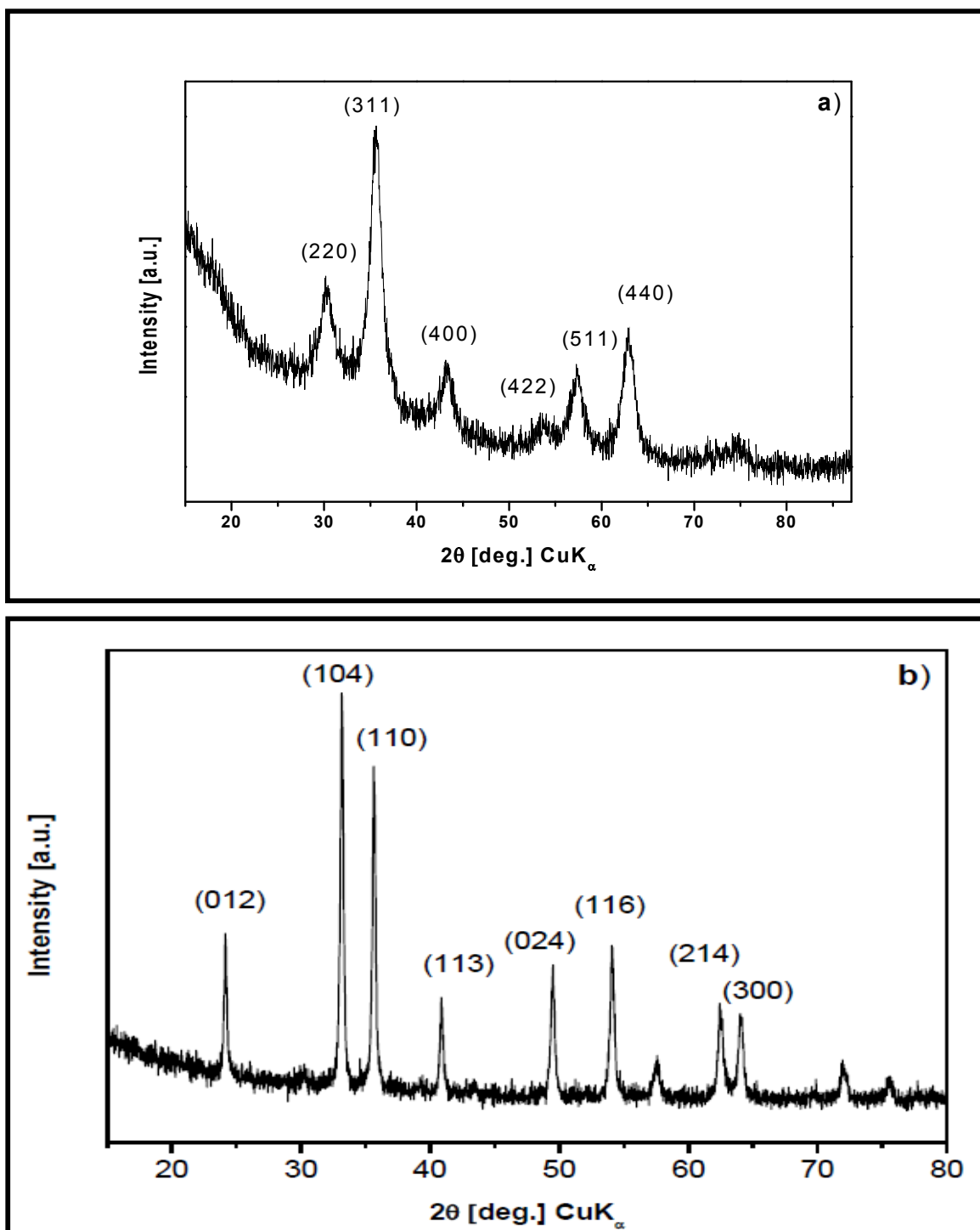
## 3. Results and discussions

### 3.1. Structural and Morphological Characterization of the Electrode Materials

Figure 1a shows the XRD pattern of the nanosized magnetite material. The pattern is indexed within the cubic Fd-3m space group typical for the spinel structure. The unit cell parameter was measured to be  $8.388(1)\text{ \AA}$ , which is closer to the value of  $8.394\text{ \AA}$  (ICDD-PDF2 #79-416) of crystalline magnetite  $\text{Fe}_3\text{O}_4$ . The analysis of the diffraction peak broadening resulted in a mean crystallite size of about 8 nm.

The powder diffraction pattern of hematite sample is presented in Figure 1b. The pattern was indexed within the rhombohedral R-3c space group. The unit cell parameters were measured to be  $a=5.0340(4)\text{ \AA}$  and  $c=13.755(2)\text{ \AA}$ , which is closer to the literature values (ICDD-PDF2 #33-664). The mean crystallite size determined for hematite sample is about 30 nm.

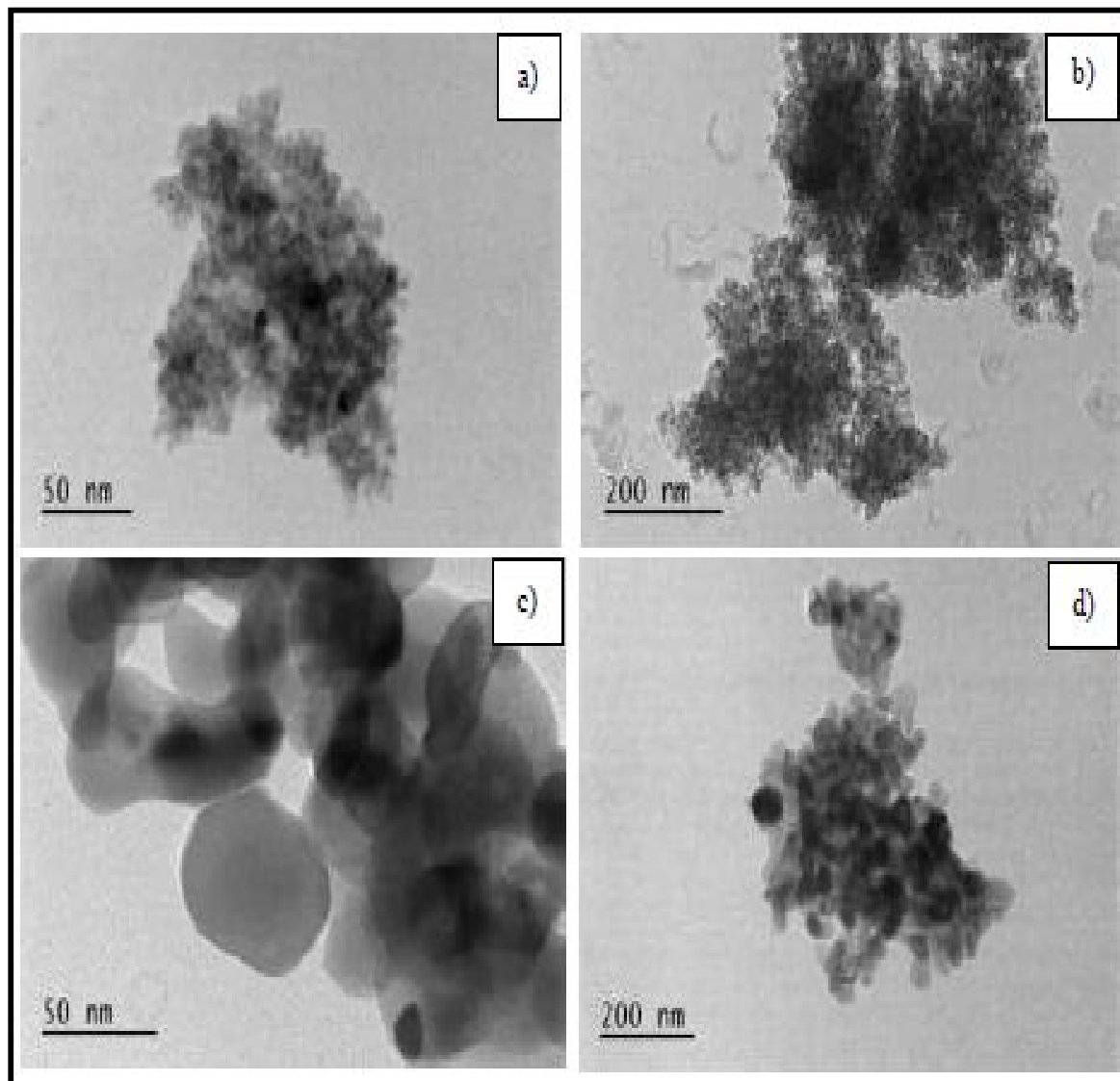
Fig 1: XRD Powder Patterns of Magnetite (A) and Hematite (B) Samples



Bright field TEM microphotographs of magnetite Fe<sub>3</sub>O<sub>4</sub> and hematite Fe<sub>2</sub>O<sub>3</sub> samples are presented in Figure 2 (a-d). The comparison of the photographs of both compounds reveals a great difference in the morphological characteristics of magnetite and hematite. These differences may be due to the different methods of synthesis. The particles of the hematite sample (Figure 2c, d) are irregular in shape with mean size about 40-50 nm. Moreover, there is a strong tendency for grouping of the individual crystallites in relatively big aggregates, which is clearly seen on the microphotograph. On the other hand, the magnetite particles (Figure 2a, b) show shape close to

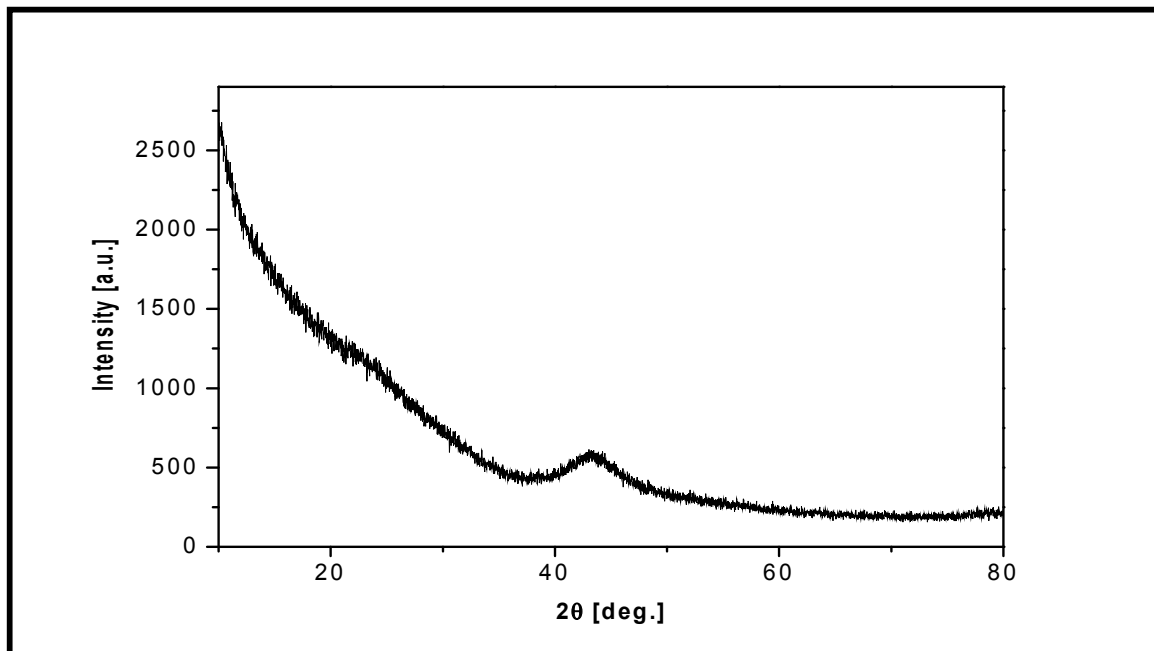
spherical, the particles are relatively small (mean size about 5-7 nm) and the individual crystallites do not aggregate.

**Fig 2: TEM Images of Magnetite (A, B) and Hematite (C, D) Samples**



XRD pattern of the activated carbon (AC) sample represents a typical pattern of amorphous material and a small hump located at around 43 degree is observed (Figure 3).

Fig 3: XRD Powder Patterns of Activated Carbon (AC) Sample

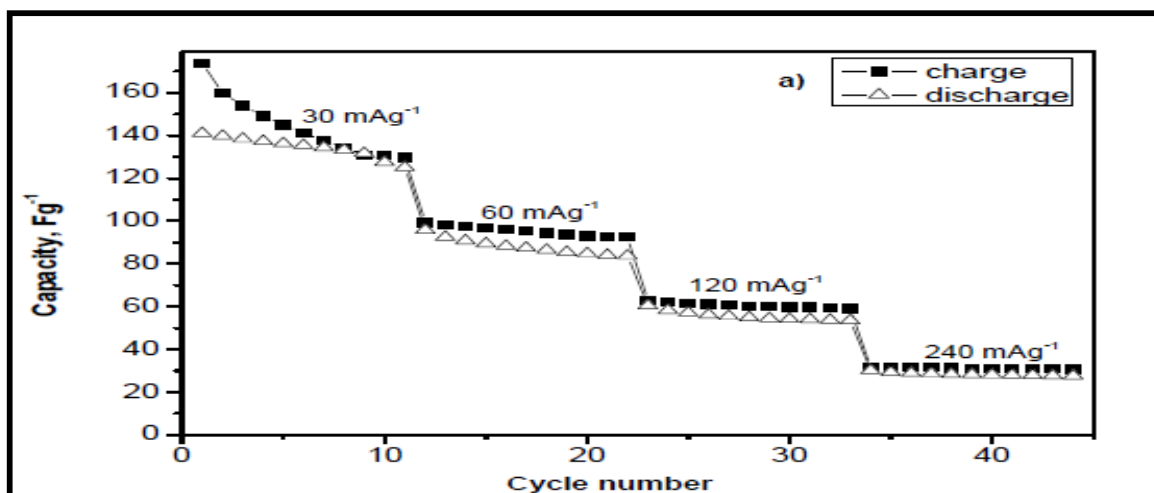


The TEM images show that the carbon particles are nanosized with large formations, separated by small clusters. The examination of the samples of activated carbon have shown that the specific surface area (BET) is  $1520 \text{ m}^2\text{g}^{-1}$ , the total volume of the pores –  $0,68 \text{ cm}^3\text{g}^{-1}$ , the volume of micropores –  $0,55 \text{ cm}^3\text{g}^{-1}$  (i.e. 80% of the total pore volume) and the average pore size - 1,8 nm [27].

The high specific surface area and high dispersion of the activated carbon material used, and all its textural parameters suggest that this carbon is an appropriate electrode material both for pure carbon electrodes in symmetric supercapacitors and for composite electrodes with carbon matrix and addition of electrochemically active compounds (e. g. oxides) in hybrid battery-supercapacitor systems.

### 1.1. Electrochemical Performance of the Supercapacitor Cells

The electrochemical performance of the symmetric and asymmetric (hybrid) capacitor cells developed are studied by charge/discharge cycling test at the same conditions, at different (increasing in values) constant current loads with minimum 10 cycles at each current rate. The main results of the cycling test of the two types of hybrid supercapacitors - with 50 wt. % magnetite or hematite addition as electrochemically active oxide in the composite carbon electrode, denoted as (AC/(LiBF<sub>4</sub> - EC/DMC 1:1) / (AC+Fe<sub>3</sub>O<sub>4</sub>)) and (AC/(LiBF<sub>4</sub> - EC/DMC 1:1)/(AC+Fe<sub>2</sub>O<sub>3</sub>)) correspondingly, are illustrated on Figure 4 (a, b).



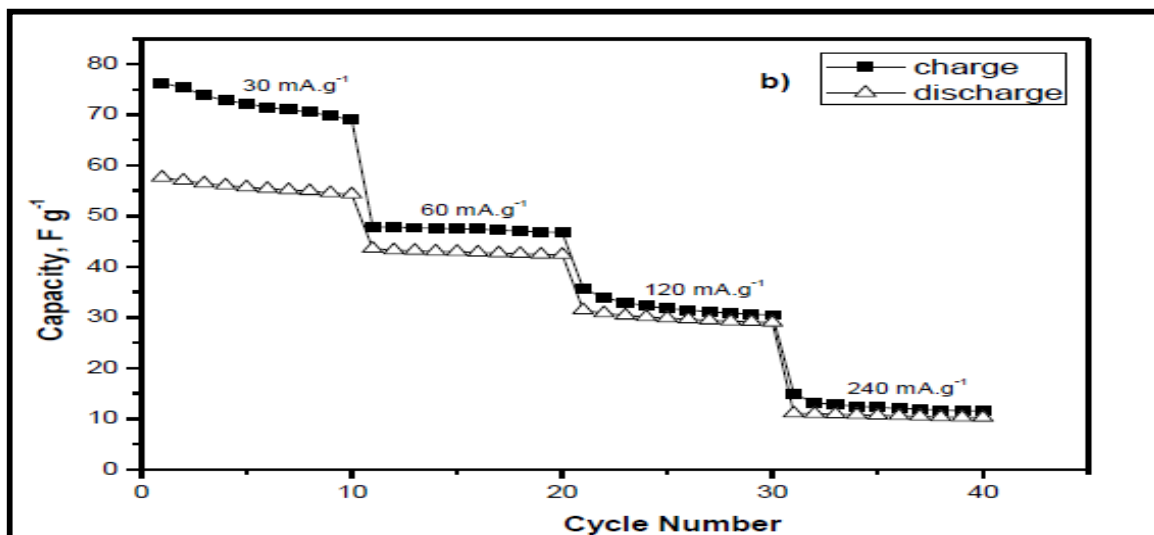


**Fig 4: Dependence of the Charge and Discharge Capacity of Hybrid Supercapacitor (AC/(LiBF<sub>4</sub> - EC/DMC 1:1)/(AC+Fe<sub>3</sub>O<sub>4</sub>)) (a) and (AC/(LiBF<sub>4</sub> - EC/DMC 1:1)/(AC+Fe<sub>2</sub>O<sub>3</sub>)) (b) on the Number of Cycles at Different Current Loads**

The analysis of the cycling behaviors shows that both hybrid supercapacitor cells demonstrate good reproducibility of the charge/discharge process and high specific discharge capacity, which is much better expressed for the magnetite based hybrid cell. The latter show about two times higher specific discharge capacity (e.g. 90 Fg<sup>-1</sup> at current load of 60 mA g<sup>-1</sup> and 30 Fg<sup>-1</sup> at 240 mA g<sup>-1</sup>) in comparison to hematite based hybrid cell (40 Fg<sup>-1</sup> at current load of 60 mA g<sup>-1</sup> and 10 Fg<sup>-1</sup> at 240 mA g<sup>-1</sup>) and this difference increases with increase of the current load. This difference in capacity obviously is related with the considerable difference in the morphology and particle size of the magnetite and hematite samples established by TEM observations (the size of the hematite particles is 8 - 10 times larger as the particles of magnetite and they form big aggregates). As expected the charge and discharge capacities decrease with increase of the current rate but the efficiency of the process (expressed as the ratio of discharge and charge capacity) increases for both hybrid cells – from an average 80% at 30 mA g<sup>-1</sup> to about 95% at 240 mA g<sup>-1</sup>. It should be noted however that the hybrid capacitor cells, especially the magnetite based cell, retain relatively high specific capacity even at very high current load (above 100 mA g<sup>-1</sup>).

The cycling behavior of a symmetric capacitor cell assembled by two identical activated carbon electrodes, at the same conditions of testing, is illustrated on Figure 6. It is established a higher specific discharge capacity for both hybrid cells in comparison to the discharge capacity of the symmetric cell, especially at low current loads (cf. the capacity data in Figure 4 a, b with those in Figure 5).

**Fig 5: Dependence of the Charge and Discharge Capacity of Symmetric Supercapacitor (AC/(LiBF<sub>4</sub> - EC/DMC 1:1)/AC) on the Number of Cycles at Different Current Loads**

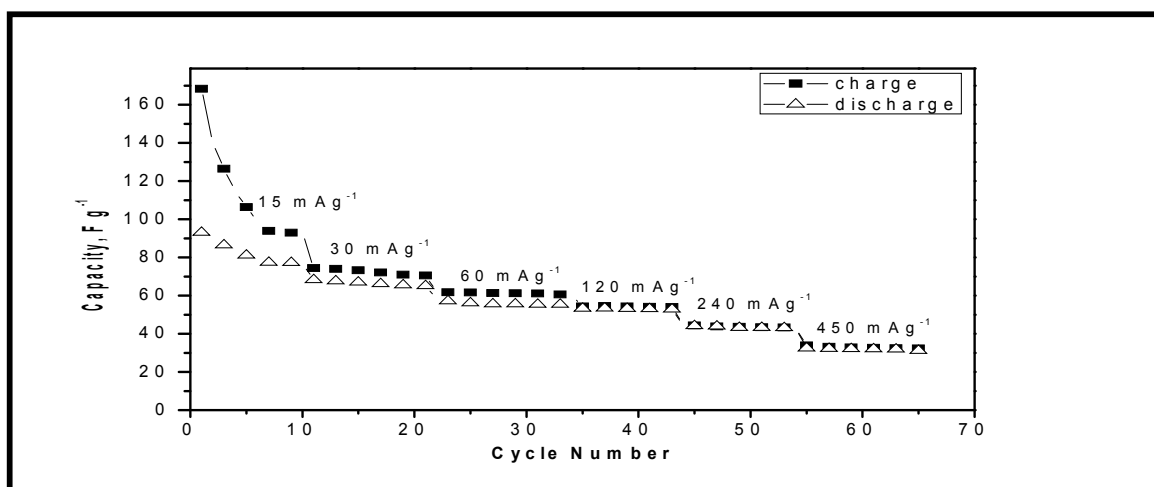
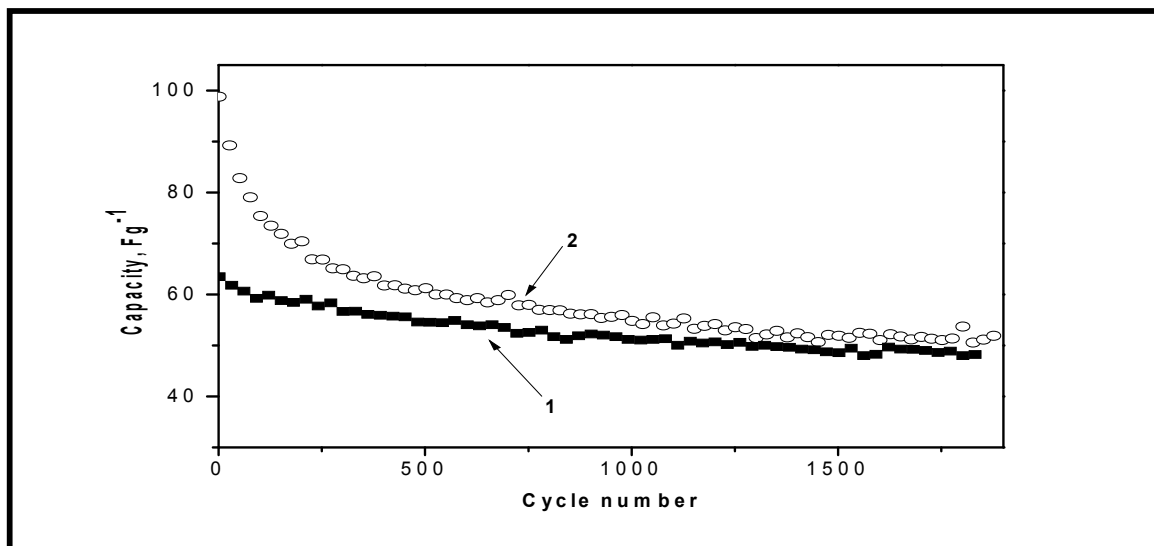


Fig. 6 shows the dependence of the discharge capacity on the number of cycles at prolong cycling (up to 2000 cycles) for the symmetric and hybrid magnetite based supercapacitors at current load of  $60 \text{ mA g}^{-1}$  for both cells. Both capacitors demonstrate high stability of the discharge capacity after prolong cycling (above 500 cycles). The hybrid supercapacitor shows 20-50% higher capacity values than that of the symmetric supercapacitor (about  $50 \text{ Fg}^{-1}$ ) and its capacity lost does not exceed 10 % after prolong cycling (above 500 cycles).

The process on the composite anodes of the hybrid cells is obviously lithiation/delithiation of  $\text{Fe}_2\text{O}_3$  or  $\text{Fe}_3\text{O}_4$  (i.e. a typical Faradaic process) together with the process of adsorption/desorption of Li-ion on the AC surface of the electrode. On the AC electrodes of the symmetric supercapacitor cell only the process of electrostatic adsorption/desorption of  $\text{BF}_4^{-1}$  takes place, i.e. the symmetric cell represents a typical electric double-layer supercapacitor for energy storage. The value of the discharge current as expected affects more strongly the capacity of the hybrid supercapacitor cell which is related to the much stronger effect of the current on the faradaic reaction on the composite electrode, i.e. on its pseudocapacity.



**Fig 6: Dependence of the Discharge Capacity of (1) Symmetric (AC/(LiBF<sub>4</sub> - EC/ DMC1:1) /AC) and (2) Hybrid Supercapacitors (AC/(LiBF<sub>4</sub> - EC/DMC 1:1)/(AC+Fe<sub>3</sub>O<sub>4</sub>)) on the Number of Cycles at Current Load  $60 \text{ mA g}^{-1}$**

The work on optimization of composition and structure of the composite electrode of the hybrid supercapacitors is in progress and the results will be reported.

## 2. Conclusions

On the basis of the results of the present study, the following conclusions could be made:

- i) Nanosized iron oxides (magnetite and hematite) are synthesized: the magnetite,  $\text{Fe}_3\text{O}_4$  - by sonochemical synthesis and the hematite,  $\text{Fe}_2\text{O}_3$  - by solution combustion synthesis. The oxides as well as the activated carbon (product of TDA Research, USA) used in the study, are structurally and morphologically characterized using XRD and TEM techniques and tested as electrode materials for hybrid supercapacitor systems.
- ii) Hybrid lithium battery-supercapacitors based on activated carbon and iron oxides is developed. The electrochemical capacitor cell is assembled with an activated carbon electrode, a composite electrode with activated carbon matrix and addition of 50 wt. %  $\text{Fe}_2\text{O}_3$  or  $\text{Fe}_3\text{O}_4$ , and non-aqueous electrolyte  $\text{LiBF}_4$ -DMC/EC (dimethyl carbonate/ethylene carbonate mixture) in ratio 1:1. Symmetric supercapacitor cell, composed by two identical electrodes of activated carbon and the same electrolyte is also assembled and tested for comparison.
- iii) The supercapacitor cells are subjected to charge/discharge cycling test under galvanostatic conditions at different current loads (from 15 to  $500 \text{ mA g}^{-1}$ ) and continuous cycling up to 2000 cycles. The hybrid supercapacitors, especially the magnetite based cell, demonstrate very good cycleability, high current efficiency which increases (up to 95%) with increase of the current load and specific capacity higher (with 20-50%) than the capacity (about  $50 \text{ Fg}^{-1}$ ) of the basic symmetric capacitor as well as stable capacity



behaviors at prolong cycling. The results prove the possibility of application of magnetite and hematite as electrochemically active material for hybrid lithium battery–supercapacitor systems.

## Acknowledgements

The financial support of the Bulgarian National Scientific Fund under project DFNI 02/18-2014 is gratefully

## References

- [1] Conway B., *Electrochemical Supercapacitors: Scientific fundamentals and technological applications*, Kluwer Academic Publ., New York, 1999.
- [2] Khomenko V., Raymundo-Piñero E., Béguin F. (2008). High-energy density graphite/AC capacitor in organic electrolyte, *Journal of Power Sources* 77, 643-651.
- [3] Zhang Y., Feng H., Wu X., Wang L., Zhang A., Xia T., Dong H., Li X., Zhang L. (2009). Progress of electrochemical capacitor electrode materials: A review, *International Journal of Hydrogen Energy* 34, 4889-4899.
- [4] Winter M., Brodd R. (2004). What Are Batteries, Fuel Cells, and Supercapacitors?, *Chemical Reviews* 104, 4245–4269.
- [5] Kötz R., Carlen M. (2000). Principles and applications of electrochemical capacitors, *Electrochimica Acta*, 45, 2483-2498.
- [6] Razumov S., Klementov A., Letvinenko S., Beliakov A., US Patent, 2001, #6, 222, 723.
- [7] Pell W., Conway B. (2004). Peculiarities and requirements of asymmetric capacitor devices based on combination of capacitor and battery-type electrodes, *Journal of Power Sources* 136, 334-345.
- [8] V. Khomenko, E. Raymundo-Piñero, F. Béguin (2006). Optimisation of an asymmetric manganese oxide/activated carbon capacitor working at 2 V in aqueous medium, *Journal of Power Sources* 153, 183-190.
- [9] Di Fabio A., Giorgi A., Mastragostino M., Soavi F. (2001). Carbon-poly (3-methylthiophene) hybrid supercapacitors, *Journal of the Electrochemical Society* 148, A845-A850.
- [10] Amatucci G., Badway F., Du Pasquier A., Zheng T. (2001). An Asymmetric Hybrid Nonaqueous Energy Storage Cell, *Journal of the Electrochemical Society* 148, A930-A939
- [11] Du Pasquier A., Plitz I., Gural J., Menocal S., Amatucci G. (2003). Characteristics and performance of 500 F asymmetric hybrid advanced supercapacitor prototypes, *Journal of Power Sources* 113, 62-71.
- [12] Mladenov M., Zlatilova P., Raicheff R., Vassilev S., Petrov N., Belov K., Trenev V., Kovacheva D. (2008). Synthesis and characterization of novel nanostructured carbon for supercapacitors on the basis of biomaterials, *Bulgarian Chemical Communications* 40, 360-366.
- [13] Petrova B., Tsyntsarski B., Budinova T., Mladenov M., Tzvetkov P. (2010). Synthesis of nanoporous carbons from mixtures of coal tar pitch and furfural and their application as electrode materials, *Fuel Processing Technology* 91, 1710-1716.
- [14] Mladenov M., Petrov N., Budinova T., Kovacheva D., Raicheff R., (2011), Synthesis and electrochemical properties of the electrode materials for supercapacitors, *Bulgarian Chemical Communications* 43, 125-131.
- [15] Mladenov M., Alexandrova K., Petrov N., Saliyski N., Raicheff R. (2013). Synthesis and electrochemical properties of activated carbons and  $\text{Li}_4\text{Ti}_5\text{O}_{12}$  as electrode materials for supercapacitors, *Journal of Solid State Electrochemistry* 17, 2101-2108.
- [16] Chen J., Xu L., Li W., Gou X. (2005).  $-\text{Fe}_2\text{O}_3$  nanotubes in gas sensor and lithium-ion battery applications, *Advanced Materials* 17, 582-586.
- [17] Zhang W., Wu X., Hu J., Guo Y., Wan L. (2008). Carbon coated  $\text{Fe}_3\text{O}_4$  nanospindles as a superior anode material for lithium-ion batteries, *Advanced Functional Materials* 18, 3941–3946
- [18] Cericola D., Kötz R. (2012). Hybridization of rechargeable batteries and electrochemical capacitors: Principles and limits, *Electrochimica Acta* 72, 1-17.

- [19] Guan D., Gao Z., Yang W., Wang J., Yuan Y., Wang B., Zhang M., Liu L. (2013). Hydrothermal synthesis of carbon nanotube/cubic Fe<sub>3</sub>O<sub>4</sub> nanocomposite for enhanced performance supercapacitor electrode material, *Materials Science and Engineering: B* 178, 736–743.
- [20] Brandt A., Balducci A. (2013). A study about the use of carbon coated iron oxide-based electrodes in lithium-ion capacitors, *Electrochimica Acta* 108, 219-225.
- [21] Mitra S., Poizot P., Finke A., Tarascon J. (2006). Growth and electrochemical characterization versus lithium of Fe<sub>3</sub>O<sub>4</sub> electrodes made by electrodeposition, *Advanced Functional Materials* 16, 2281-2287.
- [22] Cui Z., Jiang L., Song W., Guo Y. (2009). High-yield gas–liquid interfacial synthesis of highly dispersed Fe<sub>3</sub>O<sub>4</sub> nanocrystals and their application in lithium-ion batteries, *Chemistry of Materials* 21, 1162–1166.
- [23] He Y., Huang L., Cai J., Zheng X., Sun S. (2010). Structure and electrochemical performance of nanostructured Fe<sub>3</sub>O<sub>4</sub>/carbon nanotube composites as anodes for lithium ion batteries, *Electrochimica Acta* 55, 1140-1144.
- [24] Zhao X., Johnston C., Grant P. (2009). A novel hybrid supercapacitor with a carbon nanotube cathode and an iron oxide/carbon nanotube composite anode, *Journal of Materials Chemistry* 19, 8755-8760.
- [25] Yu G., Xi X., Pan L., Bao Zh., Cui Y. (2013). Hybrid nanostructured materials for high-performance electrochemical capacitors, *Nanoenergy* 2, 213-234.
- [26] Stoller M., Ruoff R. (2010). Best practice methods for determining an electrode material's performance for ultracapacitors, *Energy & Environment Science* 3, 1294-1301.
- [27] Ch. Girginov, L. Stoyanov, S. Kozhukharov, A. Stoyanova, M. Mladenov, R. Raicheff, Study on adsorption properties of carbon electrode materials for electrochemical supercapacitors, *Proceedings of scientific works of "Angel Kanchev" University of Ruse*, 54, 10.1, 2015, 89 – 95.